Journal of Saudi Chemical Society (2023) **27**, 101707

King Saud University

Journal of Saudi Chemical Society

www.ksu.edu.sa
www.sciencedirect.com

ORIGINAL ARTICLE

A theoretical approach for exploration of non-linear optical amplification of fused azacycle donor based thiophene polymer functionalized chromophores

Iqra Shafiq [a,b,1], Ume Habiba Ishaque [a,b,1], Muhammad Khalid [a,b,*], Ataualpa Albert Carmo Braga [c], Muhammad Adnan Asghar [d], Saad M. Alshehri [e], Sarfraz Ahmed [f], Suvash Chandra Ojha [g,*]

[a] *Institute of Chemistry, Khwaja Fareed University of Engineering & Information Technology, Rahim Yar Khan 64200, Pakistan*
[b] *Centre for Theoretical and Computational Research, Khwaja Fareed University of Engineering & Information Technology, Rahim Yar Khan 64200, Pakistan*
[c] *Departamento de Química Fundamental, Instituto de Química, Universidade de São Paulo, Av. Prof. Lineu Prestes, 748, São Paulo 05508-000, Brazil*
[d] *Department of Chemistry, Division of Science and Technology, University of Education Lahore, Pakistan*
[e] *Department of Chemistry, College of Science, King Saud University, Saudi Arabia*
[f] *Wellman Center for Photomedicine, Harvard Medical School, Massachusetts General Hospital, Boston, MA 02114, United States*
[g] *Department of Infectious Diseases, The Affiliated Hospital of Southwest Medical University, Luzhou 646000, China*

Received 4 April 2023; revised 19 July 2023; accepted 27 July 2023
Available online 2 August 2023

KEYWORDS

Oligothiophene;
Quantum chemical calculations;
Third order NLO;
Charge transfer;
DFT study

Abstract The quantum chemical calculations are executed for a series of designed carbazole-based oligothiophene systems (**CPTR1** and **CPTD2-CPTD8**) having D_1-π_1-D_2-π_2-A architecture. The effect of addition of π-linkers on designed architecture for the electronic and non-linear optical response was examined at M06/6-311G(d,p) level of theory. The frontier molecular orbitals (FMOs), density of states (DOS), natural population analysis (NPA), UV–Vis and transition density matrix (TDM) and non-linear optical (NLO) analyses were utilized in order to comprehend key electronic and non-linear optical response. All the designed molecules exhibited a lower energy gap (E_{LUMO}-E_{HOMO}) as 2.434–2.780 *eV*, as compared to the **CPTR1** (2.875 *eV*). Among all the derivatives, **CPTD8** exhibited the highest dipole polarizability $\langle\alpha\rangle$ and second hyperpolarizability (γ_{tot}) as

* Corresponding authors at: Institute of Chemistry, Khwaja Fareed University of Engineering & Information Technology, Rahim Yar Khan 64200, Pakistan (M. Khalid); Department of Infectious Diseases, The Affiliated Hospital of Southwest Medical University, Luzhou 646000, China (S. Chandra Ojha).
E-mail addresses: khalid@iq.usp.br (M. Khalid), suvash_ojha@swmu.edu.cn (S. Chandra Ojha).
[1] Both authors contributed equally.

Peer review under responsibility of King Saud University. Production and hosting by Elsevier.

Production and hosting by Elsevier

https://doi.org/10.1016/j.jscs.2023.101707

2.946×10^{-22} *esu* and 41.372×10^{-33} *esu*, respectively. Dipole moment (μ) and first hyperpolarizability (β_{tot}) of **CPTD8** were found to be as 3.478 *D* and 118.886×10^{-29} *esu*, correspondingly. The second hyperpolarizability (γ_{tot}) of **CPTD8** was observed to be ~6.4 ~4.0 ~2.5 ~1.8 ~1.4 ~1.3 and ~1.1 times higher in comparison to **CPTR1** and **CPTD2-CPTD7**, respectively. It is concluded that carbazole-based oligothiophene might be used as a potential material in optoelectronic devices.

1. Introduction

In the current era, non-linear optical (NLO) chromophores are designated as substantial materials owing to remarkable optoelectronic characteristics [1,2]. Advanced NLO materials innovation has significantly improved research area through the experimental and theoretical approaches [3,4]. The NLO based compounds are remarkable as a result of extensive advantages in telecommunication, optoelectronic devices, photonic tools, therapeutic testing, photoelectric materials and phosphorescent sensors [5]. The NLO active material is thoroughly based on the electronic characteristics of a molecule and the characteristics should be evaluated to examine the optical potential of the molecules [6].

In recent years, many scientific efforts have been made to explore various NLO substances involving synthetic resins, molecular dyes, organic and inorganic semiconductor diodes [7,8]. The organic compounds are selected over the other materials owing to their small dielectric constant, low cost, high photoelectric coefficients, accessibility, conjugated π-bonding system and easy electronic displacement [8,9]. In current ages, non-fullerene acceptors (NFAs) based compounds have acquired great consideration in the enhancement of organic optical response because of their powerful electron transfer capabilities [10]. NLO response also depends upon an intramolecular charge transfer (ICT) [11]. The development of ICT is entailed by donor-π-acceptor framework [12] of NLO substances manifesting "push–pull" system. The first hyperpolarizability (β_{tot}) explained by the NLO analysis relates to ICT, taking place from donor towards acceptor *via* π-conjugation [13]. In this way, the organic compounds exhibit non-linear optical properties because of the D-π-A architecture extended conjugation [14,15]. The conjugated polymers have quick response times and substantial nonlinear optical characteristics because of the existence of delocalized π-electron system [16,17]. Among these, polythiophenes are a versatile class of conjugated polymers that are attracting consideration from scientists attributed to ability of systematic structural alteration at molecular level [18]. In the literature, there was no work over the oligothiophene carbazole donor based materials in non-linear optical field. So, these molecules possessing various numbers of thiophene rings are developed from synthesized molecule (**QL1**) [19] and their structure–property relationship was explored (Scheme 1).

In the current work, eight novel oligothiophene carbazole donor based compounds (**CPTR1** and **CPTD2-CPTD8**) are analyzed computationally such as frontier molecular orbital (FMO), molecular electrostatic potential (MEP), transition density matrix (TDM), density of states (DOS) and non-linear optical (NLO) investigations. This is the first comprehensive theoretical study of azacycle-based oligothiophenes, which can be a prerequisite for developing new and better organic NLO materials.

2. Materials and methods

A new D_1-π_1-D_2-π_2-A configured azacyclic donor-based compound named as (*E*-)-3-(5-(8-(9*H*-carbazole-9-yl)phenyl)thiophen-2-yl)-2,3-dimethylquinoxalin-5-yl)thiophen-2-yl)-2-cyanoacrylic acid and abbreviated as **CPTR1** was fabricated by structural modulation of a synthesized molecule (**QL1**) [19] and optimized for selecting suitable functional for computational study. The structural alteration for designing reference molecule **CPTR1** from well-synthesized compound (**QL1**) is exhibited in Fig. 1.

For the geometry optimization of reference chromophore **CPTR1**, different DFT functionals including B3LYP [20,21]), CAM-B3LYP [22]), MPW1PW91 [23],ωB97XD [24], M06 [25] and M06-2X [26] with 6-311G(d,p) basis set [27,28] were utilized. To confirm the successful optimization of geometries, we checked the vibrational frequencies and absence of any imaginary frequency confirmed the successful optimization of our structures. The graphs in Figure S3 and tabulated dated in Tables S45-52 confirmed that the structures of entitled chromophores were at true minima. TD-DFT [29] based absorption analysis (λ_{max}) results achieved through optimized structures of aforesaid functional were found to be as 525.06, 419.37, 572.33, 421.45, 530.86 and 403.21 *nm* at M06, M06-2X, B3LYP, CAM-B3LYP, MPW1PW91 and ω B97XD, respectively. All other functionals overestimated λ_{max} magnitudes relative to M06 as λ_{max} at M06 functional was best suited with experimental data (λ_{exp} = 486 *nm*) at the aforementioned functional (λ_{DFT} = 525.06 *nm*) (Fig. 2). Subsequently, all other calculations for current study were executed at M06, because our current investigation as well as certain earlier literature described M06 efficiency [30,31]. First of all, with the aid of GaussView 6.0 software, structures of **CPTR1** and **CPTD2-CPTD8** molecules were drawn. The output files and input files of the **CPTR1** and **CPTD2-CPTD8** were generated by Gaussian 09 package [32] and GaussView 6.0 [33], respectively. From output files, results were interpreted using Avogadro [34], Chemcraft [35], GaussSum, Argus Labs [36], PyMOlyze [37] and Multiwfn 3.7. [38] The two broadly utilized methods to get transfer integrals are; Koopmans' theorem [39]) and the direct estimation method for the estimation of electronic features *via* frontier molecular orbitals (FMOs). [40]) These features are liable to study magnitude of optical response, successively interlinked to the linear response [41],⟨α⟩ and nonlinear responses [42], β_{tot} and γ_{tot}, which are first and second hyperpolarizabilities, respectively. Dipole moment (μ) and average polarizability ⟨α⟩ were estimated by Eqs. (1) and (2). While, the first hyperpolarizability (β_{tot}) and second

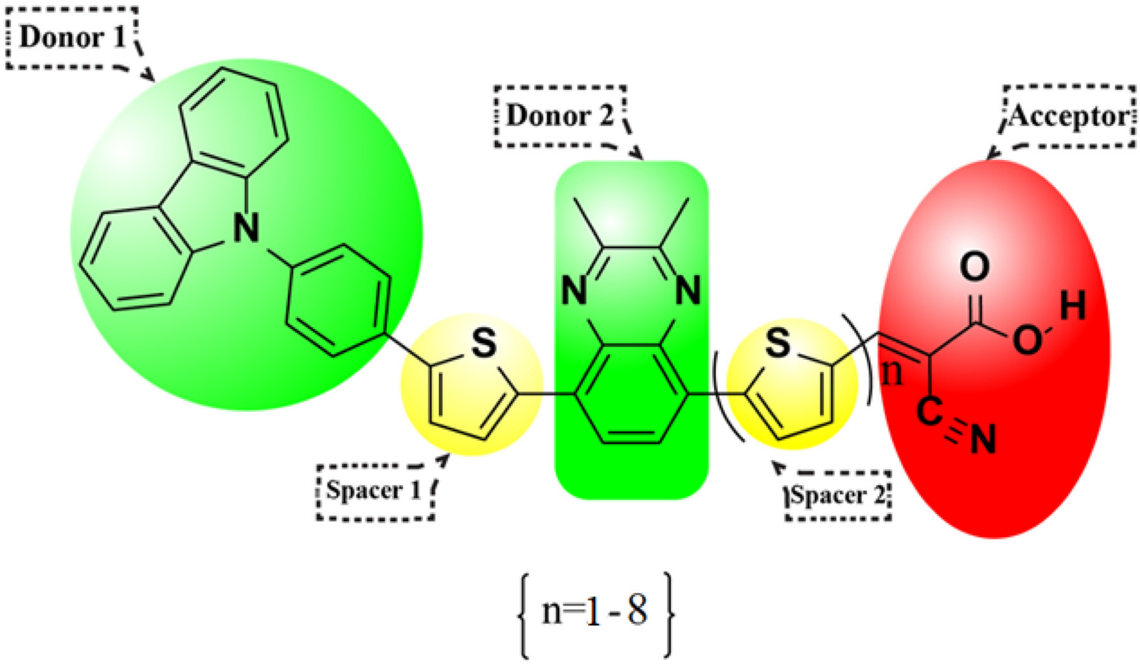

Scheme 1 A general sketch map of entitled compounds.

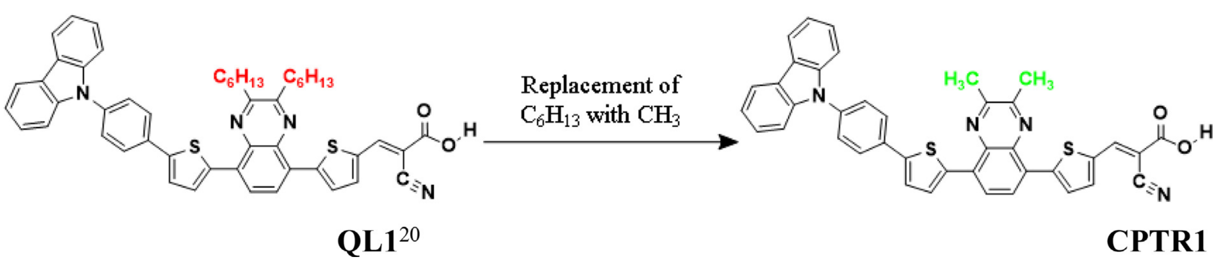

Fig. 1 Reference molecule (**CPTR1**) was obtained using parent molecule (**QL1**) *via* replacement of -C_6H_{13} with –CH_3 group.

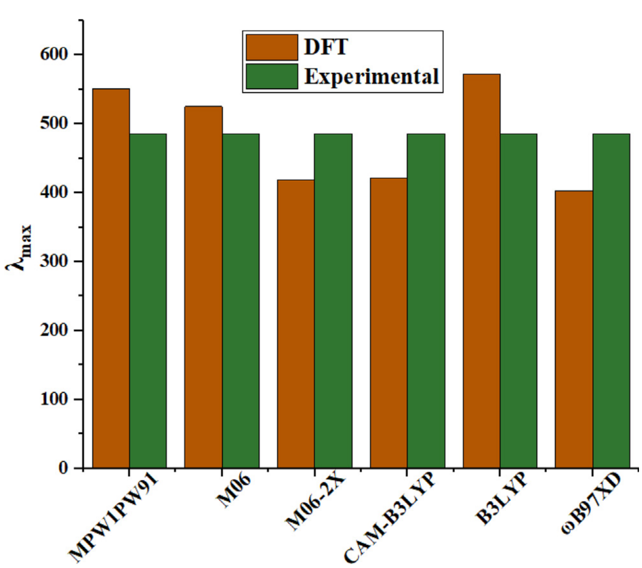

Fig. 2 Comparison of maximum absorption values of **CPTR1** between experimental and simulated values at various levels of theory: B3LYP, CAM-B3LYP, MPW1PW91, WB97XD, M06 and M06-2X at 6-311G (d,p).

hyperpolarizability (γ_{tot}) were calculated by using Eqs. (3) and (4).

$$\mu = \left(\mu[2]_x + \mu_y^2 + \mu_z^2\right)^{1/2} \quad (1)$$

$$\langle\alpha\rangle = (a_{xx} + a_{yy} + a_{zz})/3 \quad (2)$$

$$\beta_{tot} = \left(\beta_x^2 + \beta_y^2 + \beta_z^2\right)^{1/2} \quad (3)$$

Where $\beta_x = \beta_{xxx+}\beta_{xyy+}\beta_{xzz}$, $\beta_y = \beta_{yxx+}\beta_{yyy+}\beta_{yzz}$ and $\beta_z = \beta_{zxx+}\beta_{zyy+}\beta_{zzz}$

$$\gamma_{tot} = \sqrt{\gamma_x^2 + \gamma_y^2 + \gamma_z^2} \quad (4)$$

$$\gamma_i = \frac{1}{15}\sum_j (\gamma_{ijji} + \gamma_{ijij} + \gamma_{iijj}) i,j = \{x,y,z\}$$

Moreover, evaluation of various global reactivity descriptors *i.e.*, ionization potential (*IP*), global softness (σ), electron affinity (*EA*), electrophilicity index (ω), chemical potential (μ), electronegativity (X) and global hardness (η) is performed by Koopman's theorem and calculated by utilizing the Eqs. (5)–(11), respectively [39].

$$IP = -E_{HOMO} \quad (5)$$

$$EA = -E_{LUMO} \quad (6)$$

$$X = \frac{[IP + EA]}{2} \quad (7)$$

$$\eta = \frac{[IP - EA]}{2} \quad (8)$$

$$\mu = \frac{E_{HOMO}+E_{LUMO}}{2} \quad (9)$$

$$\sigma = \frac{1}{2\eta} \quad (10)$$

$$\omega = \frac{\mu^2}{2\eta} \quad (11)$$

3. Results and discussion

We have exploited **CPTR1** to fabricate seven further derivatives (**CPTD2-CPTD8**). This investigated compound was a fused five-membered azacycle (carbazole) donor-based structure acting as the first donor (D_1) named as 9-phenyl-9*H*-carbazole, thiophene ring as first π-spacer (π_1), 2,3-dimethylquinoxaline as a second donor (D_2), again the other thiophene ring is considered to be second π-spacer (π_2) and 2-cyanoacrylic acid as the acceptor (A) moiety. Structural remodeling of **CPTR1** was accomplished by introducing one thiophene unit enhanced step by step in each derivative at π_2 region, keeping rest of the structure as same in all the designed derivatives (**CPTD2-CPTD8**) and its impact on electronic, structural and NLO characteristics was explored. The structural and optimized views of entitle compounds are illustrated in Figure S1 and Fig. 3, respectively. While cartesian coordinates for entitled structures are presented in Tables S1-S8 (Supporting Information).

4. Geometric optimization

The structural parameters of **CPTR1** and **CPTD2-CPTD8** have been simulated at 6-311G(d,p) M06 level of theory using density functional theory (DFT) approach. Obtained bond lengths and bond angle values of some specific hetero-atomic functional groups are discussed and compared with published literature in order to check the accuracy of implemented computational procedure. The DFT based findings for entitled molecules are presented in Tables S9-S16 (Supplementary Information).

For compounds **CPTR1** and **CPTD2-CPTD8**, DFT based C–C bond lengths in the benzene ring are found to be in the range 1.382–1.399 Å which is in a close correspondence with the XRD bond length results for a benzene ring present in the literature 1.364–1.475 Å [43]. The corresponding values of bond length for C = O in –COOH functional group is found to be 1.2 Å by DFT. In the similar way, the C-N bond lengths in terminal cyano groups of **CPTR1** and **CPTD2-CPTD8** are observed to be same in all entitles systems as 1.155 Å. The maximum deviation value for systems: **CPTR1** and **CPTD2-CPTD8**, *via* DFT based analysis for C–C–C bond angles in the benzene ring is found in the range 117–121.1°. This result is found in close concurrence with bond angles obtained by SC-XRD as 114-124° (Tables S9-S16) [43]. Similarly, for O-C-O in –COOH, DFT computed maximum deviation in bond angles is observed to be 122.9°. In addition, the C–C-N bond angle deviation calculated *via* DFT analysis is observed to be in the range 177.5–178.3. The other findings for DFT simulated bond lengths and bond angles are presented in Tables S9-S16 (Supplementary Information).

5. Frontier molecular orbitals (FMOs) investigation

FMO investigation facilitates us to calculate notable quantum chemistry variables such as chemical stability, electronic characteristics, chemical reactivity and electron transference characteristics of examined molecules. [44]) The achieved energy difference ($E_{gap} = E_{LUMO}$-E_{HOMO}) of tailored chromophores is related to the kinetic and chemical stability. Moreover, the HOMO-LUMO energies are considered as important physical properties for determining the molecular electrical transport properties. [45] Generally, HOMO implies electron donation capability, while LUMO concentrates on the tendency of electron acceptance. [46] Compounds with larger energy gaps are supposed to be less reactive, more stable and, hard, while compounds exhibiting smaller energy gaps are regarded as strongly polarizable, soft and, unstable molecules; subsequently such molecules have magnificent NLO response. [47-49] DFT computations are employed at M06/6-311G(d,p) to demonstrate E_{LUMO}, E_{HOMO} and E_{gap} of **CPTR1** and **CPTD2-CPTD8**, and their calculated results are shown in Table 1.

Table 1 displayed the calculated HOMO/LUMO energy gap of **CPTR1** as −5.852/-2.977 *eV* with highest energy gap (2.875 *eV*). The larger energy gap found for **CPTR1** was might be because of the reduced conjugation in the system. However, reduced energy gap of (2.780, 2.674, 2.582 and 2.522 *eV*) was noted in the case of compounds, **CPTD2**, **CPTD3**, **CPTD4** and **CPTD5** relative to **CPTR1**. The observed energy gap reduction was because of adding three, four, five and six thiophene π-linkers in **CPTD2**, **CPTD3**, **CPTD4** and **CPTD5** compounds, respectively. Furthermore, the increment of π-spacers enhanced the conjugation and resulted in the reduced energy gap. The energy gap was further decreased to (2.510–2.434 *eV*) in derivatives (**CPTD6-CPTD8**) as compared to (**CPTD2-CPTD5**) due to the addition of seven, eight and nine π-bridges in these compounds. The introduction of more π-spacers resulted in increased extended conjugation which created a strong push–pull system required to get a better NLO response. The energy gap of the examined chromophores in descending order is noted as follows: **CPTR1 > CPTD2 > CPTD3 > CPTD4 > CPTD5 > CPTD6 > CPTD7 > CPTD8**. A decrease in band gap value was obtained for currently investigated chromophores from 2.780 to 2.434 *eV* through enhancement of thiophene rigs from 2 to 8 in number. From literature survey, it is revealed that enhancement of π-bridges (thiophene rings) significantly decreased the band gap and improved the charge transference rate [50]. This trend elucidates that, the introduction of additional π-spacers would be an efficient way to attain remarkable NLO behavior. [47] The charge density distribution in **CPTR1** and **CPTD2-CPTD8** on their corresponding HOMO and LUMO orbitals is displayed in Fig. 4. Appropriate charge transfer confirms

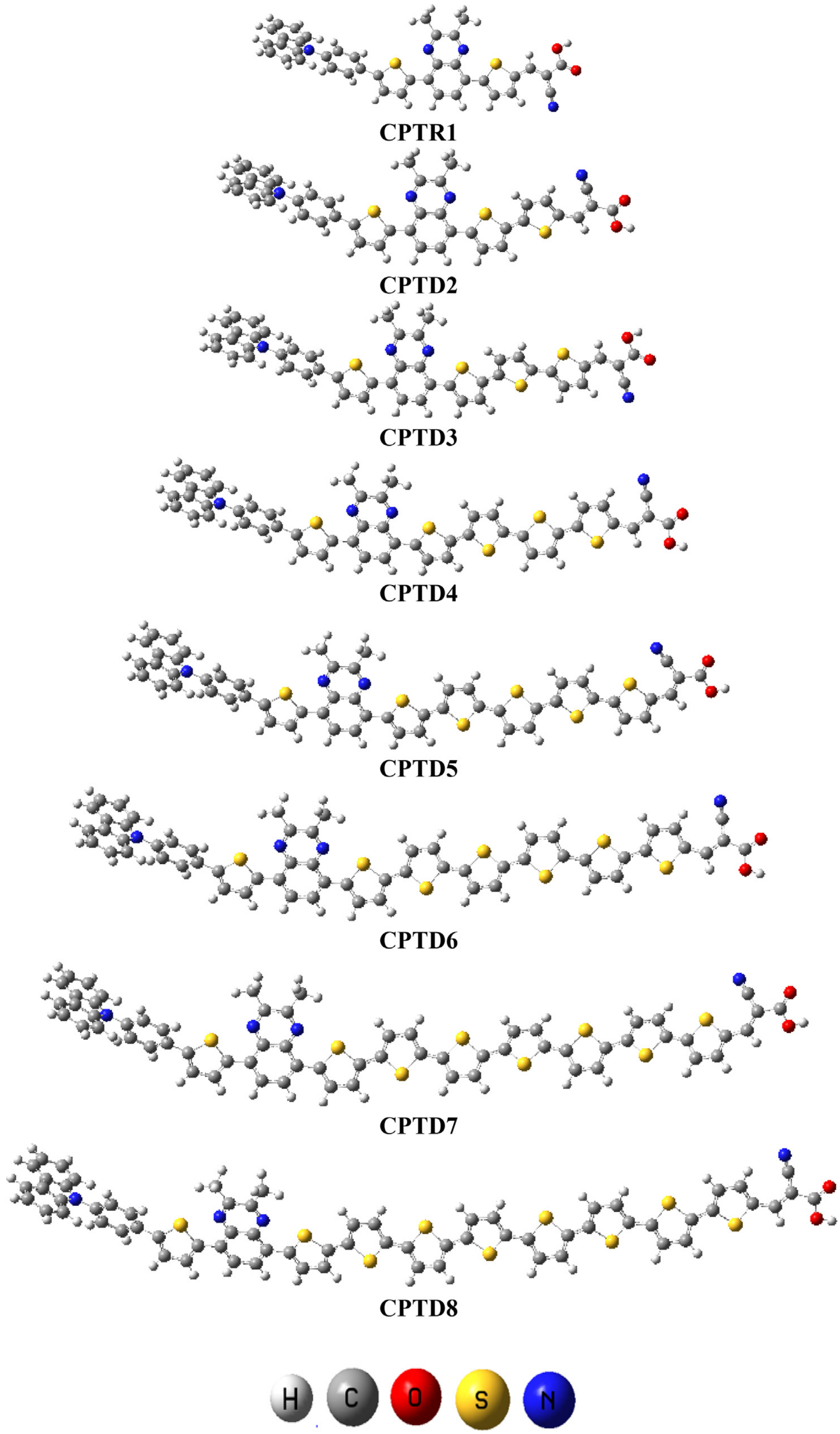

Fig. 3 Optimized structures of **CPTR1** and **CPTD2-CPTD8** with natural atomic coloring scheme.

the afore-mentioned compounds to be magnificent NLO constituents. [47,48] In reference molecule (**CPTR1**), the electronic cloud for HOMO was found significantly dispersed on the whole molecule, whereas, for LUMO it was noticeably present on D_1. However, in the tailored chromophores (**CPTD2-CPTD8**), the major portion of HOMO charge density was

Table 1 E_{HOMO}, E_{LUMO} and energy gap (E_{LUMO}-E_{HOMO}) of entitled compounds.

Chromophores	E_{HOMO}	E_{LUMO}	E_{gap}
CPTR1	−5.852	−2.977	2.875
CPTD2	−5.717	−2.937	2.780
CPTD3	−5.605	−2.931	2.674
CPTD4	−5.505	−2.923	2.582
CPTD5	−5.445	−2.923	2.522
CPTD6	−5.434	−2.924	2.510
CPTD7	−5.380	−2.921	2.459
CPTD8	−5.355	−2.921	2.434

Units in *eV*.

located over D_2 and minutely on the π-spacers. While, for LUMO, greater quantity of charge existed on terminal acceptor (A) part, while a small quantity of electronic cloud was also seen over the π_2-spacer region. The ICT originating from the donor towards the acceptor unit is illustrated by distribution between HOMO/LUMO upon compound's excitation. This electronic charge reinforcement proved that all the tailored molecules are proficient NLO active compounds.

6. Global reactivity parameters (GRPs)

DFT methodology is utilized to calculate the global reactivity descriptors *i.e.*, global softness (σ), ionization potential (*IP*), electron affinity (*EA*), electrophilicity index (ω), chemical potential (μ), electronegativity (X) and global hardness (η).

The results achieved from the Equations (6)–(12) are represented in Table 2. HOMO/LUMO energy values of investigated compounds (**CPTR1** and **CPTD2-CPTD8**) are indicated by *EA* and *IP*. Surely, electron-donating as well as electron-gaining nature of **CPTR1** and **CPTD2-CPTD8** can be determined by electron affinity and ionization potential values. [51]) Moreover, in our designed chromophores (**CPTD2-CPTD8**), the *IP* (5.355–5.717 *eV*) was found lower, relative to the reference molecule **CPTR1** (5.852 *eV*), expressing facile electron removal and less energy would be needed for polarization than **CPTR1**. The descending order of *IP* values is computed as: **CPTR1 > CPTD2 > CPTD3 > CPTD4 > CPTD5 > CPTD6 > CPTD7 > CPTD8**. Furthermore, the η values of **CPTD2-CPTD8** were observed to be much lower (1.217–1.390 *eV*) with greater σ values (0.360–0.411 *eV*) as compared to **CPTR1** (η = 1.438 *eV* and σ = 0.348 *eV*) which indicated higher chemical reactivity thus resulting in improved NLO response of studied compounds. [52] The decreasing inclination of softness was found as: **CPTD8 > CPTD7 > CPTD6 > CPTD5 > CPTD4 > CPTD3 > CPTD2 > CPTR1**. Moreover, the chemical potential is a significant element in determining the reactivity and stability of the studied compounds. As the μ values of derivatives (**CPTD2-CPTD8**) were more negative (-4.138 to −4.327 *eV* than that of reference; **CPTR1** (-4.415 *eV*), which made them kinetically less stable, chemically more reactive and highly polarizable (Table 2). The chemical potential values were in the descending trend as: **CPTD8 > CPTD7 > CPTD6 > CPTD5 > CPTD4 > CPTD3 > CPTD2 > CPTR1**. Compound **CPTD8** displayed a largest amount of electrophilicity index (ω) which confirms its electron captivating nature. The ability of an atom in a molecule to draw electrons toward itself is known as electronegativity. A molecule with a less electronegativity may be more effective as an electron transport medium because it may offer an easy removal of electrons, making it suitable to produce a high electron charge transfer. [53] The trend of electronegativity in **CPTR1 > CPTD2 > CPTD3 > CPTD4 > CPTD5 > CPTD6 > CPTD7 > CPTD8** revealed that **CPTD8** might be better as an electron transport material as compared to other entitled molecules. On the other hand, electron affinity is found lowest in **CPTD8** as compared to other studied compounds (**CPTR1-CPTD7**) which indicate that it is a compound with least accepting nature. [54] Overall, the aforementioned results demonstrated the larger charge movement tendency of entitled compounds among their HOMO and LUMO orbitals consequently resulting in improved polarizability as well as significant NLO behavior.

7. Uv–vis analysis

For evaluating the optical characteristics of the parent as well as designed compounds (**CPTR1** and **CPTD2-CPTD8**), UV/Vis absorption spectra are assessed in the gas and solvent phase *i.e.*, dichloromethane *via* utilizing M06/6-311G(d,p). UV–Vis study offers valuable computational aspects for understanding the electronic excitations, [55] contributing configurations and rate of charge shifting phenomenon within the studied molecules. [56] TD/DFT computed most prominent values of λ_{max}, excitation energy, orbitals involved in the transition and oscillator strength are demonstrated in Table 3, while rest of the results are added in Tables S17-S32 (Supporting Information). Current investigation revealed that the conjugation with prominent electron withdrawing terminal unit, hit a large bathochromic shift in UV–Vis absorption spectra. [57] The investigated complexes with D_1-π_1-D_2-π_2-A configuration, having extended π-conjugation showed interesting optoelectronic results. Higher λ_{max} value and lower transition energies were detected in all chromophores in dichloromethane as a solvent phase and tabulated in Table 3 and absorption spectra of studied compounds (**CPTR1** and **CPTD2-CPTD8**) are displayed in Fig. 5.

All the investigated molecules; **CPTR1** and **CPTD2-CPTD8**, exhibited visible region absorbance in solvent along with the gas phase. Absorption maxima of all the compounds was observed in the 537.749–609.704 *nm* range in dichloromethane. **CPTD7** compound showed maximum absorbance in the UV–Vis region, due to the presence of more extended π-conjugation and gave a λ_{max} highest peak having a value of 609.704 *nm*. Reference compound **CPTR1** displayed a minimum λ_{max} value among all the compounds, having peak value 537.749 *nm*. Decreasing order of λ_{max} was **CPTD7 > CPTD5 > CPTD8 > CPTD4 > CPTD6 > CPTD3 > CPTD2 > CPTR1** having values 609.704, 608.268, 604.974, 599.069, 598.664, 584.387, 562.334 and 537.749 *nm*, respectively. The highest value of transition energy was shown by the **CPTR1** compound (2.306 *eV*) while the lowest transition energy contribution was shown by the **CPTD7** compound (2.034 *eV*). Decreasing transition energy order was found as follows; **CPTR1 > CPTD2 > CPTD3 > CPTD6 > CPTD4 > CPTD8 > CPTD5 > CPTD7** having values 2.306, 2.205, 2.122, 2.071, 2.069, 2.049, 2.038 and 2.034 *eV*, respectively. The estimated highest peak of **CPTD7** was achieved at

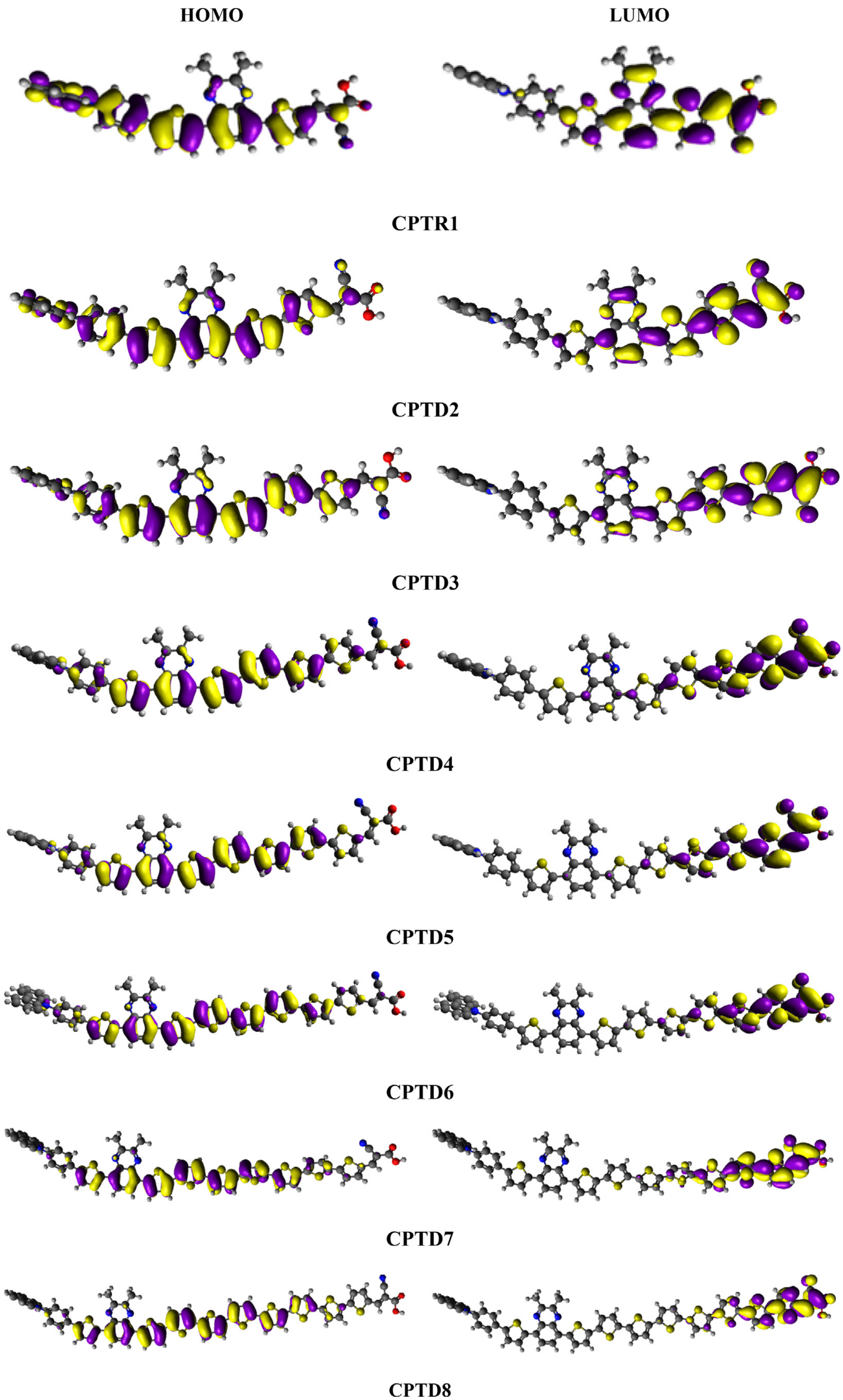

Fig. 4 HOMOs and LUMOs of **CPTR1** and **CPTD2-CPTD8.**

Table 2 Global reactivity descriptor of entitled compounds (**CPTR1** and **CPTD2-CPTD8**).

Comp.	*IP*	*EA*	*X*	*η*	*μ*	*ω*	*σ*
CPTR1	5.852	2.977	4.415	1.438	−4.415	6.778	0.348
CPTD2	5.717	2.937	4.327	1.390	−4.327	6.735	0.360
CPTD3	5.605	2.931	4.268	1.337	−4.268	6.812	0.374
CPTD4	5.505	2.923	4.214	1.291	−4.214	6.878	0.387
CPTD5	5.445	2.923	4.184	1.261	−4.184	6.941	0.397
CPTD6	5.434	2.924	4.179	1.255	−4.179	6.958	0.398
CPTD7	5.380	2.921	4.151	1.230	−4.151	7.006	0.407
CPTD8	5.355	2.921	4.138	1.217	−4.138	7.035	0.411

Units in *eV*.

Table 3 The calculated transition energies (*eV*), maximum absorption wavelengths (λ_{max}), oscillator strengths (f_{os}) and transition natures of the designed compounds.

	Comp.	λ_{max} (*nm*)	*E* (*eV*)	f_{os}	MO contributions
G[a]	**CPTR1**	524.997	2.362	1.196	H → L (90%), H-1 → L (7%)
	CPTD2	543.286	2.282	1.618	H → L (88%), H-1 → L (5%), H → L + 1 (5%)
	CPTD3	563.305	2.201	2.004	H → L (84%), H-1 → L (3%), H → L + 1 (9%)
	CPTD4	581.454	2.132	2.208	H → L (76%), H → L + 1 (16%), H-1 → L (3%)
	CPTD5	581.454	2.093	2.388	H → L (71%), H → L + 1 (20%), H-1 → L (4%)
	CPTD6	581.454	2.110	2.523	H → L (64%), H → L + 1 (22%), H-1 → L (7%)
	CPTD7	598.115	2.073	2.794	H → L (60%), H → L + 1 (23%), H-1 → L (8%)
	CPTD8	598.202	2.073	2.995	H → L (51%), H-1 → L (10%), H → L + 1 (29%)
S[b]	**CPTR1**	537.749	2.306	1.533	H → L (90%), H-1 → L (7%)
	CPTD2	562.334	2.205	1.848	H → L (89%), H-1 → L (4%), H → L + 1(4%)
	CPTD3	584.387	2.122	2.157	H → L (86%), H-1 → L (4%), H → L + 1 (8%)
	CPTD4	599.069	2.069	2.356	H → L (78%), H → L + 1 (13%), H-1 → L (5%)
	CPTD5	608.268	2.038	2.536	H → L (73%), H → L + 1 (15%), H-1 → L (6%)
	CPTD6	598.664	2.071	2.748	H → L (66%), H-1 → L (10%), H → L + 1 (17%)
	CPTD7	609.704	2.034	2.999	H → L (62%), H-1 → L (12%), H → L + 1 (17%)
	CPTD8	604.974	2.049	3.369	H → L (51%), H-1 → L (14%), H → L + 1 (22%)

MO = molecular orbital, H = HOMO, L = LUMO, f_{os} = oscillator strength, [a]gas, [b]solvent.

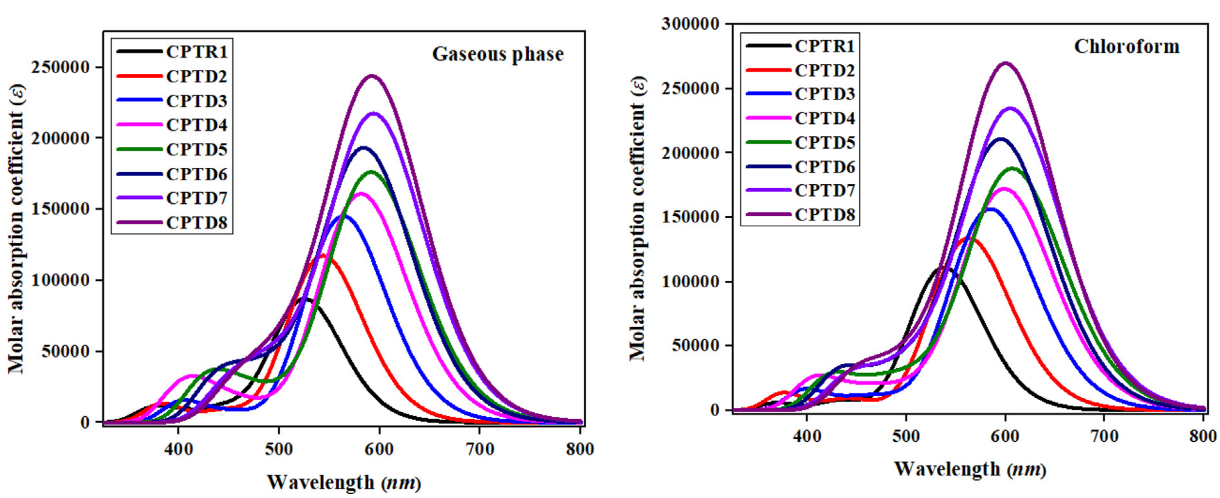

Fig. 5 UV/Vis absorption spectra of studied compounds (**CPTR1** and **CPTD2-CPTD8**) calculated at M06/6-311G(d,p) functional.

609.704 *nm* with 2.034 *eV* low transition energy and oscillator strength (2.999) showing 95% MO-contributions from HOMO to LUMO. While, calculated minimum peak for the **CPTR1** compound was attained at 537.749 *nm* with 2.306 *eV* transition energy and oscillator strength (1.533) showing 97% MO-contributions from HOMO to LUMO. Generally, wavelengths with higher value of oscillations showed stronger allowed transitions. [58] The λ_{max} values obtained for all entitled chromophores are found red shifted in dichloromethane while for gaseous phase unique pattern is noticed as λ_{max} results obtained for **CPTD4-CPTD6** are found exactly same as λ_{max} = 581.545 *nm*. Similar case was also observed for **CPTD7-CPTD8** (λ_{max} = 598.115 and 598.202 *nm* respectively) in gas phase. This might be due to geometrical parameters as in solvent phase these fabricated molecules may developed interaction with solvent molecule while in gas phase these interaction might be not possible and structures get aggregate. This unique pattern may be opened a door for scientific community in future. Nevertheless, the absorption maxima were significantly influenced by polarity alteration as well as the solvent's nature which can be confirmed by a distinct bathochromic shift in the solvent in comparison to the gas, that is greatly noticeable in donor–acceptor configured compounds. [59] As per literature assessment, molecules with lower energy gaps possess improved absorption properties, consequently higher HOMO to LUMO charge transference. [60] A decrease in excitation energy was obtained for entitled molecules from 2.306 to 2.049 *eV* after addition of thiophene rigs from 2 in **CPTR1** to 8 in **CPTD8**. The whole discussion revealed that, a low energy gap and greater charge transmission is affirmed in compounds with red shift thus, will lead to promising compounds with excellent NLO response.

8. Natural population analysis (NPA)

The Mulliken population examination is implemented to study atomic charge transformation, electronegativity equalization and electrostatic potential on the compounds under analysis. [61] The charge distribution on an atom substantially influence the chemical reactivity, dipole moment and electrostatic interfaces among the molecules and atoms. Moreover, the electronic charges perform a substantial part in bonding ability and molecular conformation. [62] Mulliken population analysis of (**CPTR1**) and its designed chromophores (**CPTD2-CPTD8**) was performed at M06/6-311G(d,p) level of theory using the DFT approach and the pictographs are displayed in Figure S2. Natural charges values for all the atoms of the entitled molecules are tabulated in Tables S37-S44.

This examination also described that the natural charge population on the electronegative atoms like C, O and N was found to be negative and a positive charge was uniformly distributed over all the hydrogen, sulfur and carbon atoms as tabulated in Tables S37-S44 (Supplementary Information). The distribution of charges depicted that the nitrogen atoms linked to oxygen atoms in entitled molecules were positively charged, while the attachment with carbon and hydrogen was accompanied by negative charges. Furthermore, all the hydrogen atoms possessed a positive charge. Oxygen atoms bonded with hydrogen and carbon atoms were found to bear a negative charge (Tables S37-S44). The general assessment of Mulliken charges discovered the unequal charge distribution over the designed chromophores owing to the carbon, nitrogen and oxygen atoms.

9. Transition density matrix (TDM) analysis

TDM investigation is utilized for determining the type of electronic transference in **CPTR1** as well as **CPTD2-CPTD8** in dichloromethane (DCM) solvent. This aids to acknowledge the nature of transition, primarily commencing ground electronic level (S_0) towards excited transition level (S_1), and communication among donor and acceptor entities attained by localization of electron-hole. [63] Impact of hydrogen (H) atom is lost owing to little involvement in transitions. Our investigated chromophores were distributed into five segments to describe the TDM results such as; donor 1 (D_1), π-spacer 1 (π_1), donor 2 (D_2), π-spacer 2 (π_2) and acceptor (A), respectively, and their heat maps are presented in Fig. 6. TDM pictographs displayed that, in reference molecule (**CPTR1**) electronic delocalization occurs on D_1, D_2 and π_1 whereas, in designed compounds, **CPTD2** and **CPTD3** the charge is significantly transferred from D_1 to D_2 through π_1 which facilitates the charge transfer without any restriction. However, in the remaining compounds *i.e.*, **CPTD4-CPTD8**, the charge density was shifted from D_1 to D_2 *via* π_1 and π_2 in a diagonal pattern.

Binding energy is a significant tool in determining optoelectronic properties of entitled compounds (**CPTR1** and **CPTD2-CPTD8**). Low binding energy results in the high charge mobility and larger NLO response. The binding energy of investigated compounds is estimated by subtracting the band gap energies from excitation energy. [64] Binding energy is calculated by utilizing Eq. (12).

$$E_b = E_{L-H}\text{-}E_{opt} \quad (12)$$

E_{opt} is the first excitation energy, E_b is the binding energy and $E_{L\text{-}H}$ is the energy gap. [65] Theoretically executed binding energies are tabulated in Table 4.

Table 4 showed that the binding energy results of all the compounds (0.575–0.385 *eV*) were smaller than the reference (0.839 *eV*). These findings revealed that, all the compounds owned a larger tendency of exciton dissociation in the excited transition state. The decreasing trend of binding energy values: **CPTR1 > CPTD2 > CPTD3 > CPTD4 > CPTD5 > CPTD6 > CPTD7 > CPTD8**. The binding energy values for investigated compounds were 0.839, 0.575, 0.552, 0.513, 0.484, 0.439, 0.425 and 0.385 for **CPTR1** and **CPTD2-CPTD8** compounds. Among all the chromophores, the lowest E_b value (0.385 *eV*) was observed in **CPTD8** which presented the greatest charge dissociation and charge transport rate.

10. Density of state (DOS) analysis

DOS investigation is executed for acknowledging the results achieved by FMOs investigation of entitled compounds (**CPTR1** and **CPTD2-CPTD8**) at the M06 functional and 6-31G(d,p) basis set. To illustrate the DOS study, we have divided the compound into five segments *i.e.*, end-capped donor 1 (D_1), π-spacer 1 (π_1), central donor 2 (D_2), π-spacer 2 (π_2) and peripheral acceptor (A) represented by red, green, blue, pink and grey lines, respectively as represented in Fig. 7. DOS uncovered the transport of electrons out of HOMO to LUMO of the compound. [64] By intruding an additional π-spacer in the designed chromophores the scattering of electronic cloud was seen migrated in various patterns around HOMO and LUMO which can be further explained by calculating DOS percentages. Herein, D_1 displayed electronic cloud scattering framework as 43.7, 23.4, 13.0, 9.1, 6.2, 5.2, 2.8 and 3.1 % to HOMO, whereas, 1.9, 0.9, 0.4, 0.2, 0.1, 0.0, 0.0 and 0.0 % to LUMO for **CPTR1** and **CPTD2-**

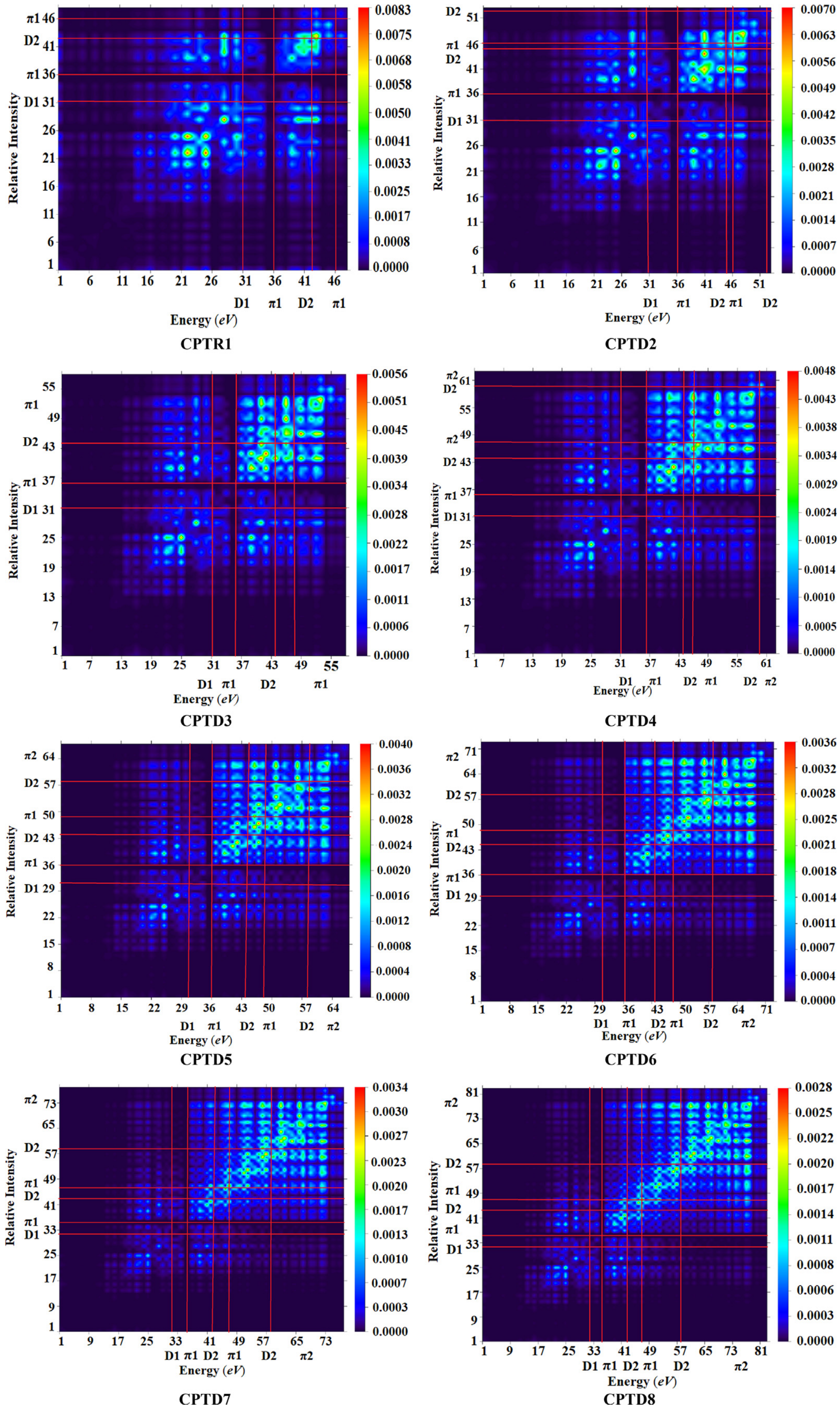

Fig. 6 TDM heat maps of studied compounds (**CPTR1** and **CPTD2-CPTD8**).

Table 4 Computed exciton binding energy (E_b) of entitled chromophores (**CPTR1** and **CPTD2-CPTD8**).

Comp.	E_{L-H}	E_{opt}	E_b
CPTR1	2.875	2.306	0.839
CPTD2	2.780	2.205	0.575
CPTD3	2.674	2.122	0.552
CPTD4	2.582	2.069	0.513
CPTD5	2.522	2.038	0.484
CPTD6	2.510	2.071	0.439
CPTD7	2.459	2.034	0.425
CPTD8	2.434	2.049	0.385

Units in *eV*.

CPTD8, respectively. However, π_1 supplied 26.2, 24.9, 19.4, 16.1, 12.4, 10.4, 6.9 and 7.0 % charge density to HOMO and 7.7, 3.8, 1.7, 0.8, 0.3, 0.1, 0.1 and 0.0 % charge density to LUMO for all the studied compounds. Similarly, D_2 was observed donating 17.6, 22.6, 21.6, 19.6, 16.5, 14.1, 10.5 and 10.4 % to HOMO while, 32.6, 16.0, 7.1, 3.1, 1.4, 0.4, 0.2 and 0.1 % electronic charge to LUMO for **CPTR1** and **CPTD2-CPTD8**, respectively. Likewise, for all the investigated compounds π_2 showed charge distribution patterns as 8.5, 25.5, 43.2, 53.6, 63.8, 69.6, 79.2 and 79.1 % for HOMO, whereas, 26.6, 44.2, 53.6, 57.1, 61.6, 59.6, 61.7 and 59.7 % to LUMO. Moreover, A exhibited electronic charge dissociation as 4.0, 3.5, 2.7, 1.6, 1.2, 0.8, 0.7 and 0.4 % to HOMO and 31.3, 35.1, 37.2, 38.9, 36.6, 39.9, 38.0 and 40.1 % to LUMO for **CPTR1** and **CPTD2-CPTD8**, respectively. These involvements favor that different types of transitions could be achieved by the introduction of additional π-spacers. In DOS diagrams, negative magnitudes along x-axis determine the valence band (HOMO) whereas, positive magnitudes indicate the conduction band (LUMO) and the space among them shows the energy gap. [66] Therefore, DOS diagrams assist the frontier molecular orbitals illustrations (see Figs. 4 and 7). Overall, DOS analysis has disclosed a proficient transference of charge density and an appreciable amount of charge is moved from D_1 to D_2 through π_1 and π_2 in the designed (**CPTD2-CPTD8**) and reference (**CPTR1**) compound.

11. Non-linear optical (NLO) analysis

Usually, organic compounds show remarkable NLO properties due to the extended conjugation system *i.e.*, low value of dielectric constant, inexpensive nature and convenient to use [67]. Therefore, they are preferably used in different areas like optical communications, optical modulation and fiber optics. [68] Moreover, NLO characteristics of organic compounds are improved by applying appropriate modifying approaches. [47,69] The NLO response corresponds to calculated values of linear polarizability ⟨α⟩, first-order hyperpolarizability (β_{tot}) and second-order hyperpolarizability (γ_{tot}) for elucidating structural and electronic properties in addition to energy gap. [70] In this way, donor and acceptor groups induce linear and nonlinear behavior of **CPTR1** and **CPTD2-CPTD8** as their ⟨α⟩, β_{tot} and γ_{tot} were computed and tabulated in Tables S33-S36 (Supporting Information) with main contributing tensors displayed in Table 5.

Among all the derivatives, **CPTD3** showed the maximum μ (3.665 *D*) due to the existence of three strongly electron-donating thiophene π-linkers which increase the conjugation and induce the polarity in the molecules [71]. Whereas, dipole moment values of **CPTR1**, **CPTD2** and **CPTD4-CPTD8** were found to be 3.717, 3.334, 3.365, 3.206, 3.206, 3.248 and 3.478 *D*, respectively. Overall, dipole moment (μ) values found decreasing in the order of: **CPTR1 > CPTD3 > CPTD8 > CPTD6 > CPTD4 > CPTD2 > CPTD7 > CPTD5**. Urea is used as a standard for the relative investigation of dipole moment. All the above-mentioned complexes hold high dipole moment values than urea (1.373 *D*). The increase in μ of all the designed molecules was found independent of the increase of π-linkers, however, it depends on the charge degree of separation among donor and acceptor moieties [72].

A careful analysis of Table 5 showed that the linear behavior was defined by average linear polarizability. Therefore, it is interesting to study the influence of increasing length of π-linkers to observe their structural and NLO properties. The average linear polarizability with its respective tensors constituents has been calculated and values in *esu* are shown in Table S34. It exposed that along α_{xx} tensor, larger values were exhibited that directed the polarization along the x-axis. However, the α_{yy} also participated notably in linear polarizability, which specified that ICT followed along the y-axis additionally. Among all, **CPTD8** showed the highest (2.946×10^{-22} *esu*) value of average linear polarizability. This might be due to an increase in electron density because of the presence of eight thiophene (π-linkers) groups. The electron density was observed to be enhanced towards acceptor moiety owing to the increment in the number of thiophene rings at π_2 region as well as due to presence of nitro and cyano substituent making it more electron-withdrawing and extending the conjugation. The descending average linear polarizability values were seen in the order: **CPTD8** > **CPTD7** > **CPTD6** > **CPTD5** > **CPTD4** > **CPTD3** > **CPTD2** > **CPTR1**.

The first hyperpolarizability (β_{tot}) also explains the NLO behavior of the compounds. The β_{tot} accompanying its contributing tensors was observed at the same level of DFT and basis set and relevant values are displayed in the Table S35. Among all the derivatives, **CPTD7** showed the highest β_{tot} amplitude (128.124×10^{-29} *esu*) with a β_{xxx} value of 122.211×10^{-29} *esu* with seven π-linkers (thiophene) at π_2 position. There is an efficient relationship established among the molecular structures and β_{tot} values. The β_{tot} factor is generally enhanced due to the substituents connected to the acceptor group, like nitro (–NO_2) and cyano (–CN) taking part in the molecular nonlinearity. Furthermore, the influence of the extended conjugated system to β_{tot} prevailed with the substitution [47]. For further clarification, the calculated results of β_{tot} of studied compounds were compared with urea ($\beta_{tot} = 0.0372 \times 10^{-29}$ *esu*) which is used as a standard molecule to analyze the NLO response [73]. The declining trend of β_{tot} for all the designed molecules in *esu* was found to be: **CPTD7 > CPTD5 > CPTD6 > CPTD8 > CPTD4 > CPTD3 > CPTD2 > CPTR1**. Among the individual tensor components, β_{xxx} exhibited the greatest values which entail better intramolecular charge transfer along x-axis.

Second hyperpolarizability γ_{tot} is an influential factor in the evaluation of NLO response [74]. The second hyperpolarizability values of aforesaid molecules with contributing tensors are revealed in the Table S36. The highest γ_{tot} value has also been

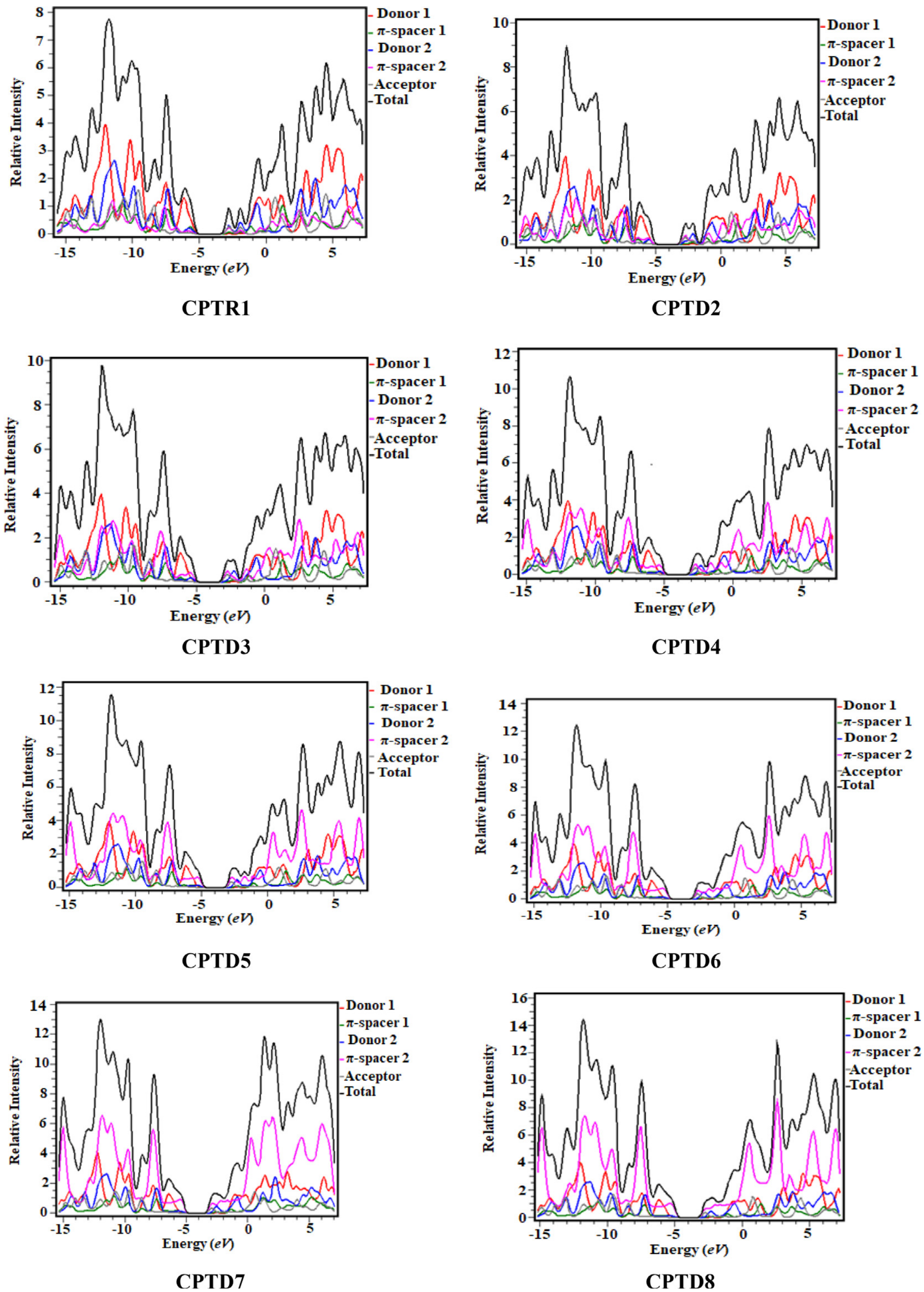

Fig. 7 DOS plots of the studied compounds, **CPTR1** and **CPTD2-CPTD8.**

recorded in **CPTD8** which is 41.371 × 10^{-33} *esu*. The γ_{tot} of all the investigated systems in *esu* falls in the order: **CPTD8** > **CPTD7** > **CPTD6** > **CPTD5 > CPTD4** > **CPTD3** > **CPTD2** > **CPTR1**. Of all the tensors, γ_x was principal and displayed extraordinarily larger values (Table S36). From the Table S36, **CPTD8** exhibited the largest γ_x value of 40.697 × 10^{-33} *esu* among all designed chromophores. This might be defined as a higher charge shifting course laterally the *x*-axis, which indicates the prominent diagonal tensor. It was concluded from the aforementioned results that electron-accepting tendency of compounds played a dynamic role and produced a remarkable nonlinear optical (NLO) response.

In order to check the efficiency of designed chromophores, a comparative analysis is made between the **CPTR1** and **CPTD2-CPTD8** and *para*-nitroaniline (*p-NA*), a popular prototypical molecule used as reference for nonlinear optical

Table 5 Computed average linear polarizability, dipole moment, first hyperpolarizability and second-order hyperpolarizability of **CPTR1-CPTD8.**

Comp.	$\mu \times 10^{-18}$	$\langle\alpha\rangle \times 10^{-22}$	$\beta_{tot} \times 10^{-29}$	$\gamma_{tot} \times 10^{-33}$
CPTR1	3.717	1.370	69.727	6.417
CPTD2	3.334	1.599	85.921	10.301
CPTD3	3.665	1.842	106.288	16.319
CPTD4	3.365	2.077	116.428	22.821
CPTD5	3.206	2.297	123.700	28.654
CPTD6	3.419	4.357	119.964	30.366
CPTD7	3.248	2.729	128.124	37.447
CPTD8	3.478	2.946	118.886	41.371

μ units in *D*, $\langle\alpha\rangle$, β_{tot} and γ_{tot} units in *esu*

activity [12]. Interestingly, designed compounds (**CPTR1** and **CPTD2-CPTD8)** showed 3.55, 4.15, 4.78, 5.39, 5.96, 1.13, 7.08, and 7.64 times greater$\langle\alpha\rangle$, respectively, then that of *p-NA* [$\langle\alpha\rangle$ = 1.178 × 10^{-23} *esu*]. Similarly, $<\gamma>$, values were found to be 2.02, 3.24, 5.12, 7.17, 9.00, 9.54, 11.76 and13.00 times greater respectively, than the standard molecule (*p-NA* = 3.182 × 10^{-36} *esu*). Furthermore, another comparative study was also done with oligothiophenes based chromophore (compound **2**) repoted by Amna *et al*. The observation revealed that the linear polarizability of all the designed derivatives was found to be 3.55, 4.15, 4.78, 5.39, 5.96, 1.13, 7.08, and 7.64 times greater, respectively, than the compound **2** [$\langle\alpha\rangle$ = 38.51 × 10^{-24} *esu*]. Furthermore, the second hyperpolarizability $<\gamma_{tot}>$ values were also found to be 0.402, 0.687, 1.087, 1.521, 1.91, 2.02, 2.50, and 2.76 times greater than the Compound **2** [$<\gamma>$ = 5.07 × 10^{-36} *esu*]. Interestingly, our compound showed good behaviour for NLO properties and can be utilized as efficient opto-electronic materials.

12. Conclusion

In summary, quantum chemical computations were accomplished for D_1-π_1-D_2-π_2-A architecture molecules (**CPTD2-CPTD8**) as designed by structural modeling of **CPTR1**. The least energy gap value among all entitled compounds was found to be 2.434 *eV* for **CPTD8**. The energy gaps of entitled compounds were obtained in descending order: **CPTR1** > **CPTD2** > **CPTD3** > **CPTD4** > **CPTD5** > **CPTD6** > - **CPTD7** > **CPTD8**. The designed compound (**CPTD8)** displayed high global softness and least global hardness as σ = 0.411and η = 1.217, respectively, as compared to the reference compound (**CPTR1**) with hardness and softness values as σ; 0.348 and η; 1.438, respectively. All the designed molecules imparted a large exciton dissociation rate due to low binding energy (E_b = 0.575–0.385 *eV*) as compared with **CPTR1** (E_b = 0.839 *eV*). Interestingly, an enhanced bathochromic shift in the absorption position of entitled compounds (λ_{max} = 562.334–609.704 *nm*) was recorded with lower transition energy (E = 2.034–2.205 *eV*). DOS and TDM investigation reinforced FMO investigation as a substantial ICT was examined from donor moiety towards acceptor unit through π-spacer. Among all the designed molecules, the lowest E_b value (0.385 *eV*) was observed in **CPTD8** which presents the greatest charge dissociation and charge transport rate. Similarly, **CPTD8** exhibited the highest linear polarizability $\langle\alpha\rangle$ and second hyperpolarizability (γ_{tot}) as 2.946 × 10^{-22} and as 41.372 × 10^{-22} *esu*. It is concluded that all the designed compounds showed better results with effective NLO response.

13. Availability of data and materials

All data generated or analyzed during this study are included in this published article and its supplementary information files.

Declaration of Competing Interest

The authors declare that they have no known competing financial interests or personal relationships that could have appeared to influence the work reported in this paper.

Acknowledgment

Dr. Muhammad Khalid gratefully acknowledges the financial support of HEC Pakistan (project no. 20-14703/NRPU/R&D/HEC/2021). Authors are thankful for cooperation and collaboration of A.A.C.B from IQ-USP, Brazil especially for his continuous support and providing computational lab facilities. A. A.C.B. acknowledges the financial support of the São Paulo Research Foundation (FAPESP) (Grants 2014/25770-6 and 2015/01491-3), the Conselho Nacional de Desenvolvimento Científico e Tecnológico (CNPq) of Brazil for academic support (Grant 309715/2017-2), and Coordenação de Aperfeiçoamento de Pessoal de Nível Superior – Brasil (CAPES) that partially supported this work (Finance Code 001). The authors thank the Researchers Supporting Project number (RSP2023R29), King Saud University, Riyadh, Saudi Arabia. The SCO acknowledges the support from the doctoral research fund of the Affiliated Hospital of Southwest Medical University.

Appendix A. Supplementary data

Supplementary data to this article can be found online at https://doi.org/10.1016/j.jscs.2023.101707.

References

[1] M.G. Papadopoulos, A.J. Sadlej, J. Leszczynski, Non-Linear Optical Properties of Matter, Springer, 2006.
[2] K. Rottwitt, P. Tidemand-Lichtenberg, Nonlinear Optics: Principles and Applications, Vol. 3, CRC Press, 2014.

[3] M. Akram, M. Adeel, M. Khalid, M.N. Tahir, M.U. Khan, M. A. Asghar, M.A. Ullah, M. Iqbal, A Combined Experimental and Computational Study of 3-Bromo-5-(2, 5-Difluorophenyl) Pyridine and 3, 5-Bis (Naphthalen-1-Yl) Pyridine: Insight into the Synthesis, Spectroscopic, Single Crystal XRD, Electronic, Nonlinear Optical and Biological Properties, J. Mol. Struct. 1160 (2018) 129–141.

[4] M.S. Ahmad, M. Khalid, M.A. Shaheen, M.N. Tahir, M.U. Khan, A.A.C. Braga, H.A. Shad, Synthesis and XRD, FT-IR Vibrational, UV–Vis, and Nonlinear Optical Exploration of Novel Tetra Substituted Imidazole Derivatives: A Synergistic Experimental-Computational Analysis, J. Phys. Chem. Solids 115 (2018) 265–276.

[5] M. Shkir, S. Muhammad, S. AlFaify, A.R. Chaudhry, A.G. Al-Sehemi, Shedding Light on Molecular Structure, Spectroscopic, Nonlinear Optical and Dielectric Properties of Bis (Thiourea) Silver (I) Nitrate Single Crystal: A Dual Approach, Arab. J. Chem. 12 (8) (2019) 4612–4626.

[6] S. Muhammad, Second-Order Nonlinear Optical Properties of Dithienophenazine and TTF Derivatives: A Butterfly Effect of Dimalononitrile Substitutions, J. Mol. Graph. Model. 59 (2015) 14–20.

[7] P.S. Halasyamani, W. Zhang, Inorganic Materials for UV and Deep-UV Nonlinear-Optical Applications, Inorganic Chemistry 56 (2017) 12077–12085.

[8] Z.H. Yang, A. Tudi, B.-H. Lei, S.L. Pan, Enhanced Nonlinear Optical Functionality in Birefringence and Refractive Index Dispersion of the Deep-Ultraviolet Fluorooxoborates, Sci China Mater 63 (8) (2020) 1480–1488.

[9] M. Anis, M. Shkir, M.I. Baig, S.P. Ramteke, G.G. Muley, S. AlFaify, H.A. Ghramh, Experimental and Computational Studies of L-Tartaric Acid Single Crystal Grown at Optimized PH, J. Mol. Struct. 1170 (2018) 151–159.

[10] D.M. Guldi, M. Maggini, G. Scorrano, M. Prato, Intramolecular Electron Transfer in Fullerene/Ferrocene Based Donor- Bridge- Acceptor Dyads, J. Am. Chem. Soc. 119 (5) (1997) 974–980.

[11] M. Adeel, M. Khalid, M.A. Ullah, S. Muhammad, M.U. Khan, M.N. Tahir, I. Khan, M. Asghar, K.S. Mughal, Exploration of CH··· F & CF··· H Mediated Supramolecular Arrangements into Fluorinated Terphenyls and Theoretical Prediction of Their Third-Order Nonlinear Optical Response, RSC Adv. 11 (14) (2021) 7766–7778.

[12] S. Muhammad, R.A. Shehzad, J. Iqbal, A.G. Al-Sehemi, M. Saravanabhavan, M. Khalid, Benchmark Study of the Linear and Nonlinear Optical Polarizabilities in Proto-Type NLO Molecule of Para-Nitroaniline, J. Theor. Comput. Chem. 18 (06) (2019) 1950030.

[13] M. Fernandes, S. S., M. Belsley, A.I. Pereira, D. Ivanou, A. Mendes, L.L. Justino, H.D. Burrows, M.M.M. Raposo, Push–Pull N, N-Diphenylhydrazones Bearing Bithiophene or Thienothiophene Spacers as Nonlinear Optical Second Harmonic Generators and as Photosensitizers for Nanocrystalline TiO2 Dye-Sensitized Solar Cells. ACS Omega 3 (10) (2018) 12893–12904.

[14] A. Mahmood, S.-U.-D. Khan, U.A. Rana, M.R.S.A. Janjua, M. H. Tahir, M.F. Nazar, Y. Song, Effect of Thiophene Rings on UV/Visible Spectra and Non-Linear Optical (NLO) Properties of Triphenylamine Based Dyes: A Quantum Chemical Perspective, J. Phys. Org. Chem. 28 (6) (2015) 418–422.

[15] A. Mahmood, M.I. Abdullah, S.-U.-D. Khan, Enhancement of Nonlinear Optical (NLO) Properties of Indigo through Modification of Auxiliary Donor, Donor and Acceptor, Spectrochim. Acta. A. Mol. Biomol. Spectrosc. 139 (2015) 425–430.

[16] M. Falconieri, R. D'Amato, A. Furlani, M.V. Russo, Z-Scan Measurements of Third-Order Optical Non-Linearities in Poly (Phenylacetylenes), Synth. Met. 124 (1) (2001) 217–219.

[17] A. Ronchi, T. Cassano, R. Tommasi, F. Babudri, A. Cardone, G.M. Farinola, F. Naso, χ (3) Measurements in Novel Poly (2′, 5′-Dioctyloxy-4, 4′, 4″-Terphenylenevinylene) Using the Z-Scan Technique, Synth. Met. 139 (3) (2003) 831–834.

[18] P. Poornesh, P.K. Hegde, G. Umesh, M.G. Manjunatha, K.B. Manjunatha, A.V. Adhikari, Nonlinear Optical and Optical Power Limiting Studies on a New Thiophene-Based Conjugated Polymer in Solution and Solid PMMA Matrix, Opt. Laser Technol. 42 (1) (2010) 230–236.

[19] K. Cai, H. Wu, T. Hua, C. Liao, H. Tang, L. Wang, D. Cao, Molecular Engineering of the Fused Azacycle Donors in the DA-π-A Metal-Free Organic Dyes for Efficient Dye-Sensitized Solar Cells, Dyes Pigments 197 (2022) 109922.

[20] B. Civalleri, C.M. Zicovich-Wilson, L. Valenzano, P. Ugliengo, B3LYP Augmented with an Empirical Dispersion Term (B3LYP-D*) as Applied to Molecular Crystals, CrystEngComm 10 (4) (2008) 405–410.

[21] G.L. Strati, J.L. Willett, F.A. Momany, A DFT/Ab Initio Study of Hydrogen Bonding and Conformational Preference in Model Cellobiose Analogs Using B3LYP/6-311 + + G, Carbohydr. Res. 337 (20) (2002) 1851–1859.

[22] T. Yanai, D.P. Tew, N.C. Handy, A New Hybrid Exchange-Correlation Functional Using the Coulomb-Attenuating Method (CAM-B3LYP), Chem. Phys. Lett. 393 (1–3) (2004) 51–57.

[23] C. Adamo, V. Barone, Exchange Functionals with Improved Long-Range Behavior and Adiabatic Connection Methods without Adjustable Parameters: The m PW and m PW1PW Models, J. Chem. Phys. 108 (2) (1998) 664–675.

[24] J.-D. Chai, M. Head-Gordon, Long-Range Corrected Hybrid Density Functionals with Damped Atom-Atom Dispersion Corrections, Phys. Chem. Chem. Phys. 10 (44) (2008) 6615–6620.

[25] V.S. Bryantsev, M.S. Diallo, A.C. Van Duin, W.A. Goddard III, Evaluation of B3LYP, X3LYP, and M06-Class Density Functionals for Predicting the Binding Energies of Neutral, Protonated, and Deprotonated Water Clusters, J. Chem. Theory Comput. 5 (4) (2009) 1016–1026.

[26] M. Walker, A.J. Harvey, A. Sen, C.E. Dessent, Performance of M06, M06–2X, and M06-HF Density Functionals for Conformationally Flexible Anionic Clusters: M06 Functionals Perform Better than B3LYP for a Model System with Dispersion and Ionic Hydrogen-Bonding Interactions, J. Phys. Chem. A 117 (47) (2013) 12590–12600.

[27] M.W. Wong, P.M. Gill, R.H. Nobes, L. Radom, 6–311G (MC) (d, p): A Second-Row Analogue of the 6–311G (d, p) Basis Set: Calculated Heats of Formation for Second-Row Hydrides, J. Phys. Chem. 92 (17) (1988) 4875–4880.

[28] J.E. Del Bene, D.H. Aue, I. Shavitt, Stabilities of Hydrocarbons and Carbocations. 1. A Comparison of Augmented 6–31G, 6–311G, and Correlation Consistent Basis Sets, J. Am. Chem. Soc. 114 (5) (1992) 1631–1640.

[29] E. Runge, E.K. Gross, Density-Functional Theory for Time-Dependent Systems, Phys. Rev. Lett. 52 (12) (1984) 997.

[30] Y. Zhao, D.G. Truhlar, The M06 Suite of Density Functionals for Main Group Thermochemistry, Thermochemical Kinetics, Noncovalent Interactions, Excited States, and Transition Elements: Two New Functionals and Systematic Testing of Four M06-Class Functionals and 12 Other Functionals, Theor. Chem. Acc. 120 (1) (2008) 215–241.

[31] S. Muhammad, H. Xu, M.R.S.A. Janjua, Z. Su, M. Nadeem, Quantum Chemical Study of Benzimidazole Derivatives to Tune the Second-Order Nonlinear Optical Molecular Switching by Proton Abstraction, Phys. Chem. Chem. Phys. 12 (18) (2010) 4791–4799.

[32] M.J. Frisch, F.R. Clemente, Gaussian 09, Revision a. 01, Mj Frisch, Gw Trucks, Hb Schlegel, Ge Scuseria, Ma Robb, Jr Cheeseman, g. Scalmani V Barone B Mennucci GA Petersson H

Nakatsuji M Caricato X Li HP Hratchian AF Izmaylov J Bloino G Zhe (2009) 20–44.

[33] R. Dennington, T.A. Keith, J.M. Millam, GaussView 6.0. 16. Semichem Inc Shawnee Mission KS USA (2016).

[34] M.D. Hanwell, D.E. Curtis, D.C. Lonie, T. Vandermeersch, E. Zurek, G.R. Hutchison, Avogadro: An Advanced Semantic Chemical Editor, Visualization, and Analysis Platform, J. Cheminformatics 4 (1) (2012) 1–17.

[35] G.A. Zhurko, Z.D.A. ChemCraft, Version 1.6, URL Httpwww Chemcraftprog Com (2009).

[36] M.A. Thompson, Molecular Docking Using ArgusLab, an Efficient Shape-Based Search Algorithm and the AScore Scoring Function, In ACS meeting, Philadelphia 172 (2004) 42.

[37] A. L. Tenderholt, PyMOlyze: A Program to Analyze Quantum Chemistry Calculations, Version 2.0. Adam Tenderholt., pymolyze. sf. net 2019.

[38] T. Lu, C. Liu, H. Duan, Q. Zeng, Mining Component-Based Software Behavioral Models Using Dynamic Analysis, IEEE Access 8 (2020) 68883–68894.

[39] T. Tsuneda, J.-W. Song, S. Suzuki, K. Hirao, On Koopmans' Theorem in Density Functional Theory, J. Chem. Phys. 133 (17) (2010) 174101.

[40] J. I. Seeman, Kenichi Fukui, Frontier Molecular Orbital Theory, and the Woodward-Hoffmann Rules. Part III. Fukui's Science and Technology, 1918–1965. *Chem. Rec.* **2022**, *22* (4), e202100302.

[41] W. Kol, os, L. Wolniewicz, Polarizability of the Hydrogen Molecule, J. Chem. Phys. 46 (4) (1967) 1426–1432.

[42] R.A. Ganeev, Nonlinear Optical Properties of Materials, Springer 174 (2013).

[43] M. Khalid, M.A. Ullah, M. Adeel, M.U. Khan, M.N. Tahir, A. A.C. Braga, Synthesis, Crystal Structure Analysis, Spectral IR, UV–Vis, NMR Assessments, Electronic and Nonlinear Optical Properties of Potent Quinoline Based Derivatives: Interplay of Experimental and DFT Study, J. Saudi Chem. Soc. 23 (5) (2019) 546–560.

[44] M. Khalid, H.M. Lodhi, M.U. Khan, M. Imran, Structural Parameter-Modulated Nonlinear Optical Amplitude of Acceptor–π–D–π–Donor-Configured Pyrene Derivatives: A DFT Approach, RSC Adv. 11 (23) (2021) 14237–14250.

[45] A.M. Dhumad, Q.M. Hassan, T. Fahad, C.A. Emshary, N.A. Raheem, H.A. Sultan, Synthesis, Structural Characterization and Optical Nonlinear Properties of Two Azo-β-Diketones, J. Mol. Struct. 1235 (2021) 130196.

[46] A. Mahmood, M.I. Abdullah, M.F. Nazar, Quantum Chemical Designing of Novel Organic Non-Linear Optical Compounds, Bull. Korean Chem. Soc. 35 (5) (2014) 1391–1396.

[47] M. Khalid, M.U. Khan, I. Shafiq, R. Hussain, K. Mahmood, A. Hussain, R. Jawaria, A. Hussain, M. Imran, M.A. Assiri, NLO Potential Exploration for D–π–A Heterocyclic Organic Compounds by Incorporation of Various π-Linkers and Acceptor Units, Arab. J. Chem. 14 (8) (2021) 103295.

[48] M. Khalid, M.U. Khan, I. Shafiq, R. Hussain, A. Ali, M. Imran, A.A. Braga, M. Fayyaz ur Rehman, M.S. Akram, Structural Modulation of π-Conjugated Linkers in D–π–A Dyes Based on Triphenylamine Dicyanovinylene Framework to Explore the NLO Properties, R. Soc. Open Sci. 8 (8) (2021) 210570.

[49] M.U. Khan, M. Khalid, I. Shafiq, R.A. Khera, Z. Shafiq, R. Jawaria, M. Shafiq, M.M. Alam, A.A.C. Braga, M. Imran, Theoretical Investigation of Nonlinear Optical Behavior for Rod and T-Shaped Phenothiazine Based D-π-A Organic Compounds and Their Derivatives, J. Saudi Chem. Soc. 25 (10) (2021) 101339.

[50] A. Bibi, S. Muhammad, S. UrRehman, S. Bibi, S. Bashir, K. Ayub, M. Adnan, M. Khalid, Chemically Modified Quinoidal Oligothiophenes for Enhanced Linear and Third-Order Nonlinear Optical Properties, ACS Omega 6 (38) (2021) 24602–24613.

[51] M. Haroon, R. Mahmood, M.R.S.A. Janjua, An Interesting Behavior and Nonlinear Optical (NLO) Response of Hexamolybdate Metal Cluster: Theoretical Insight into Electro-Optic Modulation of Hybrid Composites, J. Clust. Sci. 28 (5) (2017) 2693–2708.

[52] M.U. Khan, M. Khalid, R.A. Khera, M.N. Akhtar, A. Abbas, M.F. ur Rehman, A.A.C. Braga, M.M. Alam, M. Imran, Y. Wang, Influence of Acceptor Tethering on the Performance of Nonlinear Optical Properties for Pyrene-Based Materials with A-π-D-π-D Architecture, Arab. J. Chem. 15 (3) (2022) 103673.

[53] A.R. Chaudhry, R. Ahmed, A. Irfan, S. Muhammad, A. Shaari, A.G. Al-Sehemi, Influence of Push-Pull Configuration on the Electro-Optical and Charge Transport Properties of Novel Naphtho-Difuran Derivatives: A DFT Study, RSC Adv. 4 (90) (2014) 48876–48887.

[54] A. Hussain, M.U. Khan, M. Ibrahim, M. Khalid, A. Ali, S. Hussain, M. Saleem, N. Ahmad, S. Muhammad, A.G. Al-Sehemi, Structural Parameters, Electronic, Linear and Nonlinear Optical Exploration of Thiopyrimidine Derivatives: A Comparison between DFT/TDDFT and Experimental Study, J. Mol. Struct. 1201 (2020) 127183.

[55] A. Mahmood, Y. Sandali, J.-L. Wang, Easy and Fast Prediction of Green Solvents for Small Molecule Donor-Based Organic Solar Cells through Machine Learning, Phys. Chem. Chem. Phys. 25 (15) (2023) 10417–10426.

[56] M.U. Khan, M. Ibrahim, M. Khalid, M.S. Qureshi, T. Gulzar, K.M. Zia, A.A. Al-Saadi, M.R.S.A. Janjua, First Theoretical Probe for Efficient Enhancement of Nonlinear Optical Properties of Quinacridone Based Compounds through Various Modifications, Chem. Phys. Lett. 715 (2019) 222–230.

[57] M. Ans, J. Iqbal, K. Ayub, E. Ali, B. Eliasson, Spirobifluorene Based Small Molecules as an Alternative to Traditional Fullerene Acceptors for Organic Solar Cells, Mater. Sci. Semicond. Process. 94 (2019) 97–106.

[58] M. Khalid, M. Ali, M. Aslam, S.H. Sumrra, M.U. Khan, N. Raza, N. Kumar, M. Imran, Frontier Molecular, Natural Bond Orbital, UV-Vis Spectral Stduy, Solvent Influence on Geometric Parameters, Vibrational Frequencies and Solvation Energies of 8-Hydroxyquinoline, Int J Pharm Sci Res 8 (457.10) (2017) 13040.

[59] C. Sissa, V. Parthasarathy, D. Drouin-Kucma, M.H. Werts, M. Blanchard-Desce, F. Terenziani, The Effectiveness of Essential-State Models in the Description of Optical Properties of Branched Push-Pull Chromophores, Phys. Chem. Chem. Phys. 12 (37) (2010) 11715–11727.

[60] X. Qian, L. Lu, Y.-Z. Zhu, H.-H. Gao, J.-Y. Zheng, Triazatruxene-Based Organic Dyes Containing a Rhodanine-3-Acetic Acid Acceptor for Dye-Sensitized Solar Cells, Dyes Pigments 113 (2015) 737–742.

[61] M. Rafiq, M. Khalid, M.N. Tahir, M.U. Ahmad, M.U. Khan, M.M. Naseer, A.A.C. Braga, S. Muhammad, Z. Shafiq, Synthesis, XRD, Spectral (IR, UV–Vis, NMR) Characterization and Quantum Chemical Exploration of Benzoimidazole-Based Hydrazones: A Synergistic Experimental-Computational Analysis, Appl. Organomet. Chem. 33 (11) (2019) e5182.

[62] R.G. Parr, R.G. Pearson, Absolute Hardness: Companion Parameter to Absolute Electronegativity, J. Am. Chem. Soc. 105 (26) (1983) 7512–7516.

[63] M. Ans, J. Iqbal, Z. Ahmad, S. Muhammad, R. Hussain, B. Eliasson, K. Ayub, Designing Three-Dimensional (3D) Non-Fullerene Small Molecule Acceptors with Efficient Photovoltaic Parameters, ChemistrySelect 3 (45) (2018) 12797–12804.

[64] M. Khalid, I. Shafiq, M. Zhu, M.U. Khan, Z. Shafiq, J. Iqbal, M.M. Alam, A.A.C. Braga, M. Imran, Efficient Tuning of Small Acceptor Chromophores with A1-π-A2-π-A1 Configuration for High Efficacy of Organic Solar Cells via End Group Manipulation, J. Saudi Chem. Soc. 25 (8) (2021) 101305.

[65] M. Khalid, M.U. Khan, E. -Razia, Z. Shafiq, M.M. Alam, M. Imran, M.S. Akram, Exploration of Efficient Electron Acceptors for Organic Solar Cells: Rational Design of Indacenodithiophene Based Non-Fullerene Compounds, Sci. Rep. 11 (1) (2021) 19931.

[66] T. Lu, F. Chen, Multiwfn: A Multifunctional Wavefunction Analyzer, J. Comput. Chem. 33 (5) (2012) 580–592.

[67] M. Khalid, M.U. Khan, R. Hussain, S. Irshad, B. Ali, A.A.C. Braga, M. Imran, A. Hussain, Exploration of Second and Third Order Nonlinear Optical Properties for Theoretical Framework of Organic D–π–D–π–A Type Compounds, Opt. Quantum Electron. 53 (2021) 1–19.

[68] J. Iqbal, I.S. Yahia, H.Y. Zahran, S. AlFaify, A.M. AlBassam, A.M. El-Naggar, Linear and Non-Linear Optics of Nano-Scale 2′, 7′ Dichloro-Fluorescein/FTO Optical System: Bandgap and Dielectric Analysis, Opt. Mater. 62 (2016) 527–533.

[69] M.N. Arshad, I. Shafiq, M. Khalid, A.M. Asiri, Exploration of the Intriguing Photovoltaic Behavior for Fused Indacenodithiophene-Based A-D–A Conjugated Systems: A DFT Model Study, ACS Omega 7 (14) (2022) 11606–11617.

[70] M. Khalid, M.N. Arshad, S. Murtaza, I. Shafiq, M. Haroon, A. M. Asiri, S.F. de AlcântaraMorais, A.A. Braga, Enriching NLO Efficacy via Designing Non-Fullerene Molecules with the Modification of Acceptor Moieties into ICIF2F: An Emerging Theoretical Approach, RSC Adv. 12 (21) (2022) 13412–13427.

[71] P. Piyakulawat, A. Keawprajak, K. Jiramitmongkon, M. Hanusch, J. Wlosnewski, U. Asawapirom, Effect of Thiophene Donor Units on the Optical and Photovoltaic Behavior of Fluorene-Based Copolymers, Sol. Energy Mater. Sol. Cells 95 (8) (2011) 2167–2172.

[72] S. Muhammad, H. Xu, Z. Su, K. Fukuda, R. Kishi, Y. Shigeta, M. Nakano, A New Type of Organic-Inorganic Hybrid NLO-Phore with Large off-Diagonal First Hyperpolarizability Tensors: A Two-Dimensional Approach, Dalton Trans. 42 (42) (2013) 15053–15062.

[73] D.R. Kanis, M.A. Ratner, T.J. Marks, Design and Construction of Molecular Assemblies with Large Second-Order Optical Nonlinearities. Quantum Chemical Aspects., Chem. Rev. 94 (1) (1994) 195–242.

[74] T.J. Marks, M.A. Ratner, Design, Synthesis, and Properties of Molecule-Based Assemblies with Large Second-Order Optical Nonlinearities, Angew. Chem. Int. Ed. Engl. 34 (2) (1995) 155–173.